

# HRTEM STUDY OF CARBONS PREPARED BY HTT OF UNBURNED CARBON FROM COAL COMBUSTION FLY ASHES

*Jean-Noël Rouzaud, Laboratoire de Géologie, ENS, CNRS, 24, rue Lhomond 75231, Paris cedex 5, France  
Miguel Cabiellés and Ana B. García, INCAR (CSIC), Francisco Pintado Fe 26, 33011 Oviedo, Spain*

## Introduction

Fly ashes are solid wastes produced in coal combustion plants. These wastes need to be disposed of and/or reused. Coal fly ashes disposal in dumps lead to several environmental problems, while the reusing is limited by the proportion of unburned carbon remaining what can amount up to 15-20 wt. %. The unburned carbon from coal combustion fly ashes shows high carbon contents (> 80 %) and a structure with a certain degree of tridimensional order. Based on this and due to the presence of metallic species able to act as catalysts, unburned carbon appears as a potential precursor for the preparation of synthetic graphite. In this work, carbon materials with a high degree of structural order were obtained by heating a concentrate of unburned carbon from coal combustion fly ashes in the temperature range of 1800-2700 °C. The interlayer spacing,  $d_{002}$ , and crystallite sizes along the c axis,  $L_c$ , and the a axis,  $L_a$ , calculated from XRD, as well as the Raman parameters, relative intensity of the D Raman band (attributed to defects),  $I_D/I_G$ , and width of the G band (attributed to graphite),  $W_G$ , were employed to follow the evolution with the temperature of the overall degree of structural order of the carbon materials prepared. High-resolution transmission electron microscopy (HRTEM) was used to image directly the profile of the polyaromatic layers, and thus the improvement of the graphitization. By coupling HRTEM with local elemental analyses by Energy Dispersive Spectroscopy, the transformations with the temperature of the inorganic matter (mainly iron and silicon) of the unburned carbon concentrate were evidenced. The presence of these elements seems to be responsible for the high structural degree of the materials prepared.

## Experimental section

Fly ashes were collected from a pulverized coal combustion plant in the north-west of Spain. This particular coal combustion plant is mainly fed with anthracites. A concentrate of unburned carbon, denoted CVP, with an unburned carbon mean content of 54.6 wt.%, was obtained from the fly ashes by screening out the  $\leq 80 \mu\text{m}$  fraction. The HTT experiments of the CVP sample were carried at 1800-2700 °C in a graphite furnace for 1 h under an argon flow followed by cooling to room temperature also under argon flow. The heating rates for HTT were 20 °C  $\text{min}^{-1}$  from room temperature to 2000 °C and 10 °C  $\text{min}^{-1}$  from 2000 °C to the prescribed temperature. The carbon materials thus prepared were identified by the precursor designation (CVP) and the HTT temperature, such as CVP/2000.

Structural characterization of the materials comprises XRD and Raman measurements. The X-ray diffractograms of the samples were recorded in a Siemens model D5000 powder diffractometer that was equipped with monochromatic Cu  $K\alpha$  X-ray source and had an internal standard of silicon powder. Diffraction data were collected by step scanning with a step of 0.02 °  $2\theta$  and a scan step time of 1 s. For each sample, five diffractograms were obtained, using a different representative batch of sample for each run. The interlayer spacing,  $d_{002}$ , was calculated from the position of the (002) peak applying Bragg's equation. The crystallite sizes along the c-axis,  $L_c$ , and along a-axis,  $L_a$ , were calculated from the (002) and (110) peaks, respectively, using the Scherrer formula, with values of  $K=0.9$  for  $L_c$  and 1.84 for  $L_a$ , respectively [Warren, B. E. et al. 1965]. The broadening of diffraction peaks due to instrumental factors was corrected with the use of a silicon standard. Raman spectra were obtained in a HR 800 Jobin Yvon Horiba system using the green line of an argon laser ( $\lambda = 514.5 \text{ nm}$ ) as excitation source and equipped with a CCD camera. The  $\times 100$  objective lens of an Olympus M Plan optical microscope was used both to focus the laser beam (at a power of approx 25 mW) and to collect the scattered radiation. Extended scans from 1225 to 1700  $\text{cm}^{-1}$  and 2500-2900  $\text{cm}^{-1}$  were respectively performed to obtain the first- and second-order Raman bands of the samples with typical exposure times of 30 s. In order to assess differences within samples, at least 21 measurements were performed on different particles of each individual sample. The intensity (I) and the width (W) of the bands were measured using a mixed Gaussian-Lorentzian curve-fitting procedure. Four synthetic graphites GS1-4 were also analyzed for comparative purpose.

HRTEM has been carried out on a Jeol 2011 microscope equipped with a LaB<sub>6</sub> gun and operating at 200 kV. Magnification up to 400 kx was necessary to observe the lattice fringe of both graphitic and disordered carbons. The resolution in the lattice fringe mode is 0.14 nm. Local elemental analyses by Electron Dispersive Spectroscopy (EDS) mode has been performed thanks to a PGT energy selective X-ray analyzer allowing in situ analysis on volumes smaller than 100  $\text{nm}^3$ , with a precision of 1%. The samples were firstly grounded, dispersed in ethanol and a drop of solution was then deposited on a classical TEM copper grid, previously covered by a holey amorphous carbon film. Examination of the sample was focused on parts of the samples laying across the holes to obtain information free of the contribution of the supporting carbon film.

## Results and discussion

### *Materials structural order: effect of temperature*

The interlayer spacing  $d_{002}$ , the crystallite sizes  $L_c$  and  $L_a$ , and the Raman parameters, relative intensity of the D-band  $I_D/I_t$  ( $I_t = I_G + I_D + I_{D'}$ ) and width of the G band  $W_G$  of the carbon materials prepared from the precursor CVP are reported in **Table 1**. Data corresponding to the reference graphites GS1-4 are also collected in this table. Experimental errors are not included in the table for clarity. Typical standard errors of crystallite sizes are <2% and <8% of the values reported for  $L_c$  and  $L_a$ , respectively. The  $d_{002}$  values are much more precise, with standard errors of <0.1%. The average intensities of the Raman bands were calculated with errors <6%.

**Table 1.** XRD Crystalline and Raman  $I_D/I_t$  and  $W_G$  parameters of the materials prepared and reference graphites

Material	$d_{002}$ (nm)	$L_c$ (nm)	$L_a$ (nm)	$I_D/I_t$ (%)	$W_G$ ( $cm^{-1}$ )
CVP/1800	0.3416	8.5		44.7	33.4
CVP/2000	0.3411	9.5		33.0	28.9
CVP/2200	0.3391	15.7		23.8	23.5
CVP/2300	0.3383	22.9		16.4	19.8
CVP/2400	0.3382	18.9		16.4	19.4
CVP/2500	0.3387	19.5	51.5	15.3	20.1
CVP/2600	0.3384	20.0	51.8	12.4	19.7
CVP/2700	0.3385	19.0	50.3	11.9	19.7
Graphite GS1	0.3359	25.8	47.4	12.9	18.6
Graphite GS2	0.3367	36.6	62.7	14.3	18.0
Graphite GS3	0.3374	33.6	63.0	28.7	17.7
Graphite GS4	0.3379	21.7	53.2	10.3	15.1

The degree of the structural order of the carbon materials that have been prepared from CVP tends to increase as the treatment temperature increases (see **Table 1**). However, two temperature zones may be distinguished in the evolution of the degree of crystallinity of these materials: (i) 1800-2400 °C and (ii) >2400 °C. Thus, as the treatment temperature increases from 1800 °C to 2400 °C, the interlayer spacing  $d_{002}$  decreases quickly to reach a plateau value of approximately 0.338 nm. In a similar way, a growth of the crystallite size  $L_c$ , particularly at temperatures above 2000 °C occurs. Basically, no significant improvement in the average degree of structural order of the materials as determined by XRD parameters was attained at temperatures above 2400 °C. As an example, crystallite thickness values in the c direction  $L_c$  of 19.5, 20.0 and 19.0 nm were calculated for the materials CVP/2500, CVP/2600 and CVP/2700, respectively. The trend followed by the Raman parameters  $I_D/I_t$  and  $W_G$  of the materials, relative to the precursor treatment temperature, is similar to that of XRD parameters (**Table 1**). The decay of these parameters indicates an improvement of the crystallite size of the materials prepared [Cuesta, A. et al. 1998; Zerda, w. et al. 2000]. On the basis of the Raman data, the second temperature zone clearly starts at temperature above 2500 °C with a plateau value of ~ 12 %.

According to the XRD crystalline parameters in **Table 1**, the HTT of the unburned carbon concentrate studied at temperatures  $\geq 2300$ -2400 °C results in carbon materials that have structural order degrees comparable to those of some synthetic graphites what are commercially available. These graphites are currently employed in several industrial applications, such as anode material in lithium-ion batteries (GS3) and electrical conductor for the cathode in alkaline batteries (GS4). As shown by the values of the crystallite size  $L_c$ , the structural differences between the reference synthetic graphites and the materials prepared are mainly related to the less-developed three-dimensional order of the later. Comparison with the Raman data makes clear some additional differences. The  $W_G$  values of some of the graphites are narrower than those of the materials, thus indicating larger coherent domains at least on the surface (the depth of the laser beam penetration in carbons can be evaluated to be about 0.2  $\mu m$ ) of the reference graphites. These differences in the graphitic order seem to be related to the higher coherent domains  $L_c$  of the graphites, rather than being affected by the larger values of  $L_a$ . In fact, the ratio  $I_D/I_t$ , which has been used as an indicator of the 'bidimensional crystallite order' of the materials [Angoni, K. 1998; Beny, C. et al. 1985; Cuesta, A. et al. 1998; Tuinstra, F. et al. 1970], is greater in some reference graphites (see GS3 in **Table 1**). It is important to mention that, apart from the crystal size, there are other factors that have been suggested to contribute to the Raman D band intensity, such as the presence of amorphous/disordered carbon or doping [Cuesta, A. et al. 1998], thus explaining the lower value of  $I_D/I_t$  calculated for the graphite GS4 as compared to that of the material CVP/2600 material with apparently similar degree of structural order as determined by XRD. Therefore, the information provided by XRD seems to be inconclusive in determining whether or not small noticeable amounts of disordered or even amorphous carbon are present in a given material.

### HRTEM and EDS characterization

Unlike XRD what gives averaged structural data, HRTEM allows looking the sample heterogeneity, specifically the presence of disordered carbon phases and/or large crystals of graphite

Small crystallites (*more properly named Basic Structural Units or BSUs*) with preferential planar orientation were observed by HRTEM to be present in the precursor CVP (**Figure 1a**). This type of precursor lamellar microtexture was previously related to its ability to graphitize [Rouzaud, J. N. et al. 1989; Blanche, C. et al. 1995]. The following main features of the CVP precursor structural changes under HTT are shown by HRTEM:

(1) The formation of graphite as well as polygonal graphite structures after heating the precursor at even the lowest temperature of 1800 °C (**Figure 1b, c and e**). Graphitic domains with thickness in the c direction  $L_c$  of ~14-19 nm and ~23-26 nm were calculated with the ImageJ software in several graphite structures found by HRTEM in the CVP/1800 and CVP/2000 materials, respectively; these values being higher than those determined by XRD (**Table 1**). The presence in these materials of disordered carbon phases is responsible of the difference in the  $L_c$  values. So, XRD appears to be less sensitive than HRTEM to determine the graphitic domains dimensions of the materials prepared at temperature up to 2000 °C. XRD technique only accounts for the perfect domains, while HRTEM also images more or less wrinkled stacks of layers, as shown by the presence of Bragg fringes which appear normally to the graphene layers.

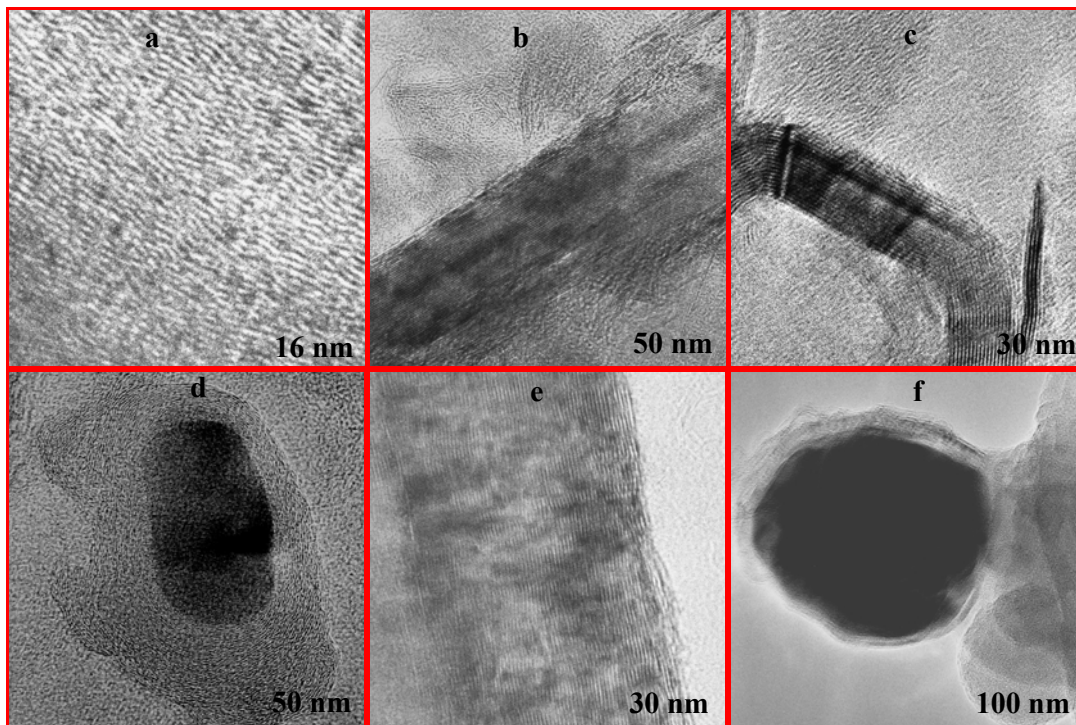


**Figure 1.** HRTEM images showing the 002 lattice fringe of CVP precursor (a), the material CVP/1800 material (b, c, d) and CVP/2000 material (e, f)

(2) The presence of structures in which crystallized inorganic impurities phases are surrounded by parallel carbon sheets in the materials prepared at 1800 °C and 2000 °C (**Figure 1d and f**). Iron and a compound of iron/silicon were identified by EDS as the inorganic species appearing in the structures of **Figure 1d** and **1f**, respectively. Similar structures were previously found to appear during the HTT of coals as a consequence of the catalytic effect of the mineral impurities [Oberlin, A. et al. 1975; Evans, E. L. et al. 1972]. By subsequent heat-treatment, these structures lead to the formation of metal carbides which further decomposition leaves at least partially graphitized *hollow shells* with carbon layers parallel to the external surface.

(3) Structures that clearly correspond to polycrystalline graphite (with dotted electron diffraction patterns, see Figure 2b) were identified in the material prepared at 2200 °C (**Figure 2a and b**). Values of  $L_c$  of ~ 20 nm were calculated for these graphites from the HRTEM images. Mineral impurities (iron) surrounded by parallel carbon layers structures were not detected in CVP/2200 material. Unlike iron, silicon was identified by EDS to be present together with carbon in several particles of this material (**Figure 2c**). Following a model proposed to explain the catalytic graphitization of coals during heat-treatment [Oberlin, A. 1971], the active constituents (metals, mainly Fe and Si) of

the coals mineral matter would react during HTT with the disordered carbons to form carbides; their further decomposition leading to graphitic carbons. So, it seems that well crystallized silicon carbide is still present in CVP/2200 material, its corresponding SAED pattern appearing in **Figure 2d**.

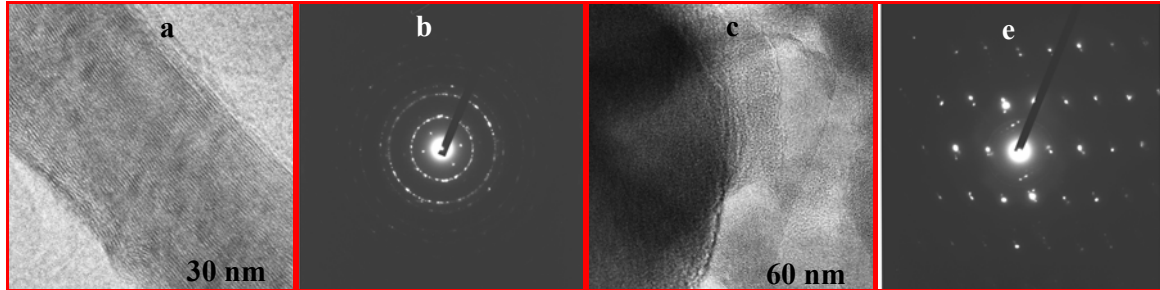


**Figure 2.** HRTEM images of CVP/2200 material: (a) graphitised carbon, (b) SAED pattern of the graphitised carbon, (c) silicon/carbon particle and (d) SAED pattern of the silicon/carbon particle

(4) Mainly graphite-like structures, several of them polygonal, were observed by HRTEM in the material prepared at 2400 °C (**Figure 3a and b**). Unlike in those obtained at lower temperatures, the average value of the crystallite size  $L_c$  measured directly from several graphite images is similar to that calculated by XRD (**Table 1**). According to the EDS analysis of the HRTEM images of different particles of CVP/2400 (**Figure 2c**), silicon is the main inorganic element remaining in this material. As mentioned above for CVP/2200, it appears together with carbon and well crystallized (**Figure 2d**), thus inferring the presence of silicon carbide.

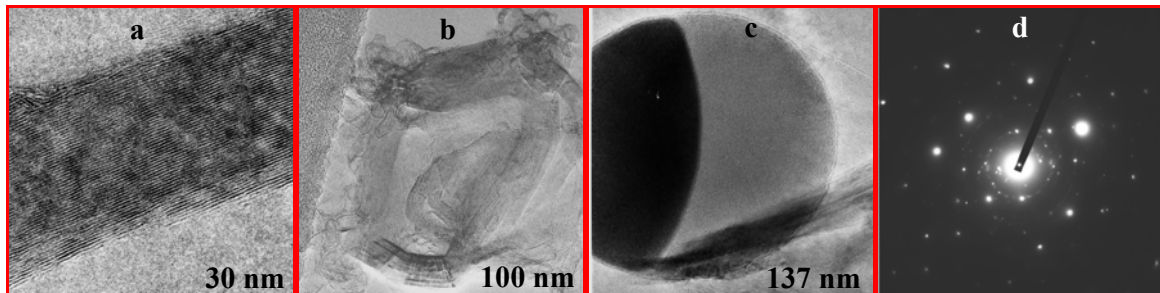


**Figure 3.** HRTEM images of CVP/2400 material: (a) graphitic structure, (b) polygonal graphite, (c) silicon/carbon particle and (d) SAED pattern of the silicon/carbon particle

(5) *Stricto sensu* graphite structures with a very high degree of layers parallelism and almost no defects were found in CVP/2700 material (**Figures 4a and b**); their electron diffraction pattern correspond to graphite (**Figure 4d**). Values of  $L_c$  of  $\sim 44$  nm were measured for these graphite structures, thus suggesting the progress of the graphitization a temperatures beyond 2400 °C. In addition, some very large crystals were observed under the dark field mode (**Figure 4c**), their SAED pattern corresponding to large and superimposed crystals of graphite lying on the 001 plane (**Figure 4d**). As in the material prepared at 2400 °C, well crystallized silicon/carbon particles were observed.

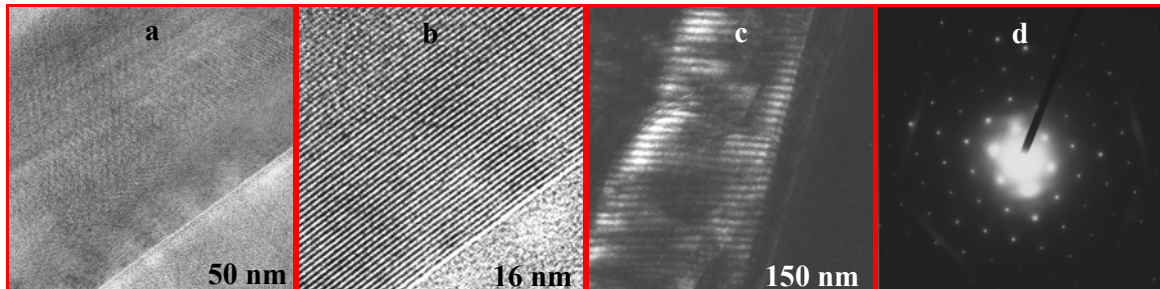


**Figure 4.** HRTEM images of CVP/2700 material: (a) and (b) graphite structure at different enlargements, (b) crystal structure under *dark field* mode and (d) SAED pattern of the crystal appearing in c

## Conclusions

- The microstructural changes occurring during the high temperature treatment of a concentrate of unburned carbon from coal combustion fly ashes have been successfully monitored by means X-ray diffraction, Raman spectroscopy and HRTEM.
- As shown by the XRD and Raman parameters, carbon materials with significant degree of structural order were prepared from the unburned carbon concentrate at temperatures  $\geq 2400$  °C. However, *stricto sensu* graphite structures were only observed by HRTEM in the material prepared at 2700 °C.
- The presence of some mineral impurities, specifically iron and silicon, in the unburned carbon concentrate seems to be responsible for the high degree of structural order of the material prepared. Different mineral crystallized phases such as iron, iron/silicon and silicon/carbon were identified in the materials prepared by coupling HRTEM with EDS.

## References

- Angoni, K. 1998. A study of highly ordered carbon by use of macroscopic and microscopic Raman spectroscopy. *Journal of Materials Science* 33:3693-3698.
- Beny, C. and J. N. Rouzaud. 1985. Characterization of carbonaceous materials by correlated electron and optical microscopy and Raman microspectroscopy. Pages 119-132 in *Scanning Electron Microscopy, SEM Inc., AMF O'Hare*, Chicago. USA.
- Blanche, C., J. N. Rouzaud and D. Dumas. 1995. New data on anthracite graphitizability. Pages 694-695 in *Proceedings of 22<sup>nd</sup> Biennial on Carbon*. American Carbon Society, San Diego. USA.
- Cuesta, A., Dhameincourt, P., Laureyns, Martínez-Alonso and J. M. D. Tascón. 1998. Comparative performance of X-ray diffraction and Raman microprobe techniques for the study of carbon materials. *Journal of Materials Chemistry* 8:2875-2879.
- Evans, E. L., J. L. Jenkins and J. M. Thomas. 1972. Direct electron microscopic studies of graphitic regions in heat-treated coals and coal extracts. *Carbon* 10:637-642.
- Oberlin, A. and J. P. Rouchy. 1971. Transformation des carbones non graphitisables par traitement thermique en présence de fer. *Carbon* 9 :39-46.
- Oberlin, A. and G. Terriere. 1975. Graphitization studies of anthracites by high resolution electron microscopy. *Carbon* 13:367-376.
- Rouzaud, J. N. and A. Oberlin. 1989. Structure, microtexture and optical properties of anthracene and saccharose-based carbons. *Carbon* 27:517-529.
- Tuinstra, F. and J. L. Koenig. 1970. Raman spectrum of graphite. *The Journal of Chemical Physics* 53:1126-1130.
- Warren, B. E. and P. Bodenstein. 1965. The diffraction pattern of fine particles carbon blacks. *Acta Crystallographica* 18:282-286.
- Zerda, W. and T. Gruber. 2000. Raman study of kinetics of graphitization of carbon blacks. *Rubber Chemistry and Technology* 73:289-292

**Acknowledgment.** Financial support from the Spanish Ministry of Education and Science, MEC (under Projects MAT2001-1843 and MAT2004-01094) and FICYT (under Project PB-EXP01-01) is gratefully acknowledged. One of the authors (A. B. Garcia) thanks the Spanish Ministry of Education for a personal grant of the Spanish Scientists Mobility Program (ref. PR2005-0201).